Nuclear Medicine and Biology 39 (2012) 1081–1086

Contents lists available at SciVerse ScienceDirect

Nuclear Medicine and Biology

journal homepage: www.elsevier.com/locate/nucmedbio

Ex Vivo and *In Vivo* Evaluation of the Norepinephrine Transporter Ligand [^{11}C]MRB for Brown Adipose Tissue Imaging

Shu-fei Lin [a], Xiaoning Fan [b], Catherine Weikart Yeckel [c], David Weinzimmer [a], Tim Mulnix [a], Jean-Dominique Gallezot [a], Richard E. Carson [a], Robert S. Sherwin [b], Yu-Shin Ding [a,*]

[a] *PET Center, Department of Diagnostic Radiology, Yale University, New Haven, CT 06520, USA*
[b] *Department of Internal Medicine, Yale University, New Haven, CT 06520, USA*
[c] *John B. Pierce Lab, New Haven, CT 06520, USA*

ARTICLE INFO

Article history:
Received 1 February 2012
Received in revised form 6 April 2012
Accepted 15 April 2012

Keywords:
Norepinephrine transporter
[^{11}C]MRB, (S,S)-O-[^{11}C]methylreboxetine
Brown adipose tissue
PET imaging

ABSTRACT

Introduction: It has been suggested that brown adipose tissue (BAT) in humans may play a role in energy balance and obesity. We conducted *ex vivo* and *in vivo* evaluation using [^{11}C]MRB, a highly selective NET (norepinephrine transporter) ligand for BAT imaging at room temperature, which is not achievable with [^{18}F]FDG.
Methods: PET images of male Sprague–Dawley rats with [^{18}F]FDG and [^{11}C]MRB were compared. Relative [^{18}F]FDG or [^{11}C]MRB retention at 20, 40 and 60 min post-injection was quantified on awake rats after exposing to cold (4 °C for 4 h) or remaining at room temperature. Rats pretreated with unlabeled MRB or nisoxetine 30 min before [^{11}C]MRB injection were also assessed. The [^{11}C]MRB metabolite profile in BAT was evaluated.
Results: PET imaging demonstrated intense [^{11}C]MRB uptake (SUV of 2.9 to 3.3) in the interscapular BAT of both room temperature and cold-exposed rats and this uptake was significantly diminished by pretreatment with unlabeled MRB; in contrast, [^{18}F]FDG in BAT was only detected in rats treated with cold. *Ex vivo* results were concordant with the imaging findings; i.e. the uptake of [^{11}C]MRB in BAT was 3 times higher than that of [^{18}F]FDG at room temperature ($P = 0.009$), and the significant cold-stimulated uptake in BAT with [^{18}F]FDG (10-fold, $P = 0.001$) was not observed with [^{11}C]MRB ($P = 0.082$). HPLC analysis revealed 94%–99% of total radioactivity in BAT represented unchanged [^{11}C]MRB.
Conclusions: Our study demonstrates that BAT could be specifically labeled with [^{11}C]MRB at room temperature and under cold conditions, supporting a NET-PET strategy for imaging BAT in humans under basal conditions.

1. Introduction

Obesity is characterized by impaired energy expenditure associated with adaptive thermogenesis [1–4]. Brown adipose tissue (BAT) is one of the primary tissues responsible for adaptive non-shivering thermogenesis in mammals [5] and it contributes to energy expenditure. Previously, BAT was thought to disappear in humans as a part of development into adulthood. However, cold-induced, high-level uptake of 2-[^{18}F]-fluoro-D-deoxy-D-glucose([^{18}F]FDG) in the supraclavicular fossa, axillae, and neck has been repeatedly observed during clinical PET scanning. These observations lifted the veil on the continued existence of BAT in adult human. Subsequent investigation has verified the existence of BAT by tissue biopsy [6,7]. Unlike white adipose tissue (WAT) which has been long regarded as an energy storage organ, and more recently, as a major secretory and endocrine organ releasing adipokines involved in a wide range of functions [8], the relative importance of BAT activity to adult human whole-body energy expenditure is still unknown. To better characterize the role of BAT in energy balance of obesity in humans, a non-invasive PET imaging approach is needed.

Based on [^{18}F]FDG-PET imaging data, BAT metabolic activity is related to age, gender, BMI, cold exposure and medications [6]. Studies have shown that [^{18}F]FDG-imaging requires subjects under cold stimulation during the PET imaging, and BAT does not appear to be visualized with [^{18}F]FDG-PET at room temperature [9,10]. Thus, the [^{18}F]FDG-PET approach may not be suitable for imaging BAT at the basal state, i.e., at room temperature. Since BAT activation appears to be dynamic, expressing large variability due to thermal sensitivity, individual differences in BAT activation due to variations in thermal response are likely to make comparisons between obese and normal weight subjects difficult. Moreover, [^{18}F]FDG is not specific to BAT, nor is glucose the primary substrate for BAT heat production. The [^{18}F]FDG-PET strategy will not address regulatory mechanisms that are related to the specific sympathetic nervous system (SNS) modulation

* Corresponding author. PET center, New York University School of Medicine, New York, NY 10016. Tel.: +1 212 263 6605; fax: +1 212 263 7541.
E-mail addresses: yushin.ding@nyu.edu, yu-shin.ding@nyumc.org (Y.-S. Ding).

0969-8051/$ – see front matter © 2012 Elsevier Inc. All rights reserved.
doi:10.1016/j.nucmedbio.2012.04.005

features of BAT, which are likely to be key features to understanding potential dysfunction [1–5]. Therefore, it is important to develop new and more specific methods to address both the plasticity of BAT activation and basal characteristics that do not require stimulation or that could alternatively be used in combination with strategies that highlight BAT stimulated activity.

The purpose of this study was to test a new, mechanistically driven approach for potential imaging of BAT in humans that capitalizes on the fact that BAT is strongly innervated and regulated by the SNS machinery. More specifically, we imaged the norepinephrine recycling component, designated the norepinephrine transporter (NET) with [^{11}C]MRB ((S,S)-O-[^{11}C]methylreboxetine), a highly selective NET ligand. We have previously shown [^{11}C]MRB to label brain regions innervated by norepinephrine neurons in humans (subjects with cocaine dependence and attention deficit hyperactivity disorder (ADHD)) [11–14], as well as in non-human primates (NHP) [15], including imaging peripheral tissues with high NET [16].

Rats were used to establish the new method because rodents are known to have a large amount of BAT in the interscapular region [17,18]. In this study, we conducted both e*x vivo* and *in vivo* evaluation to systematically compare the capability of [^{11}C]MRB and [^{18}F]FDG for imaging the presence, distribution, mass, and activity of BAT. That is, we directly compared labeling of interscapular BAT between [^{11}C]MRB and [^{18}F]FDG in awake rats under room temperature and cold exposure conditions. We also determined the detection capability NET-PET imaging for the interscapular BAT in anesthetized rats, as compared to[^{18}F]FDG-PET imaging, under both conditions.

The specificity of [^{11}C]MRB uptake in BAT was further assessed both *ex vivo* and *in vivo* by pretreatments with unlabeled MRB or nisoxetine (a selective NET-inhibitor) in order to determine the fraction of specific binding to NET. The metabolite profile and the chemical form in BAT after injection of[^{11}C]MRB were also evaluated.

2. Methods

2.1. Radiotracers

[^{11}C]MRB was synthesized at Yale PET center as described previously [15] and [^{18}F]FDG was purchased from IBA Molecular (Dulles, VA, USA).

2.2. Animals

Male Sprague–Dawley rats (290–320 g, Charles River, Richmond, VA) aged from nine to eleven weeks were individually housed in the temperature (22–23 °C) and humidity controlled rooms in the Yale Animal Resources Center. The animals were fed rat chow (Agway Prolab 3000, Syracuse, NY) and water *ad libitum* and were acclimatized to handling at a 12:12-h light–dark cycle (lights on between 0700 and 1900) for a period of 1 week before the vascular catheter implantation. Under isoflurane anesthesia, vascular catheters [PE50 tubing with a tip made from silastic laboratory tubing (0.51 mm inner diameter)] were inserted via a neck incision into the internal jugular vein and carotid artery and extended to the level of the right atrium and aortic arch, respectively. All animals were allowed to have one week recovery from the surgery before tracer injections. The animal care and experimental protocols were reviewed and approved by the Yale Institutional Animal Care and Use Committee.

2.3. PET Imaging

The effects of cold exposure on the uptake of [^{18}F]FDG (series 1) and [^{11}C]MRB (series 2), and the specific binding of [^{11}C]MRB in BAT (series 3) were assessed by PET scans. A microPET Focus-220 (Siemens, Knoxville, TN, USA) was used. Two rats were used in each series and placed side by side. In series 1 and 2, one rat was wrapped with a pad at room temperature; another was maintained at 4 °C for 4 h before tracer injection and was wrapped with cold packs (4 °C). PET emission data were acquired with 5 min × 3 bed positions at 45 min post-injection of [^{18}F]FDG in series 1. For [^{11}C]MRB, emission acquisition was acquired in 3 bed positions over a period of ~100 min.

The same imaging protocol of series 2 was applied to a blocking study (series 3) on two rats which received either saline solution or unlabeled MRB solution (2 mg/kg) at 30 min prior to [^{11}C]MRB injection (unlabeled MRB at a dose of 1 mg/kg has been shown to significantly block [^{11}C]MRB binding in non-human primates (unpublished results)). For each series, the transmission scan was obtained after emission scans with 3 matched bed positions, 9 min each. The animals were kept anesthetized using isoflurane gas during the PET acquisitions.

2.4. Ex vivo Biodistribution Study

Awake male Sprague–Dawley rats were administered [^{18}F]FDG or [^{11}C]MRB intravenously via the vascular catheters after exposing to cold (4 °C for 4 h, $n=9$) or remaining at room temperature (22–23 °C, $n=9$) and were sacrificed by lethal injection of pentobarbital at 20, 40 and 60 min post-injection. Another set of rats was pretreated intravenously with saline ($n=12$) or 2 mg/kg of unlabeled MRB ($n=8$) or nisoxetine ($n=4$) 30 min before [^{11}C]MRB injection and was sacrificed at 40 or 60 min after injection. Samples were collected immediately from blood (either through the vascular catheter or directly from the heart), BAT (the major depot in the interscapular area), abdominal WAT, brain, heart, skeletal muscle, lung, liver, kidney, bone and pancreas and were counted in a cross-calibrated well counter (Wizard 1480, Perkin Elmer, Waltham, MA, USA) and weighed. Relative tracer retention of excised tissues was quantified in units of %ID/g. Analysis of variance (ANOVA) and mean separations by Fisher's least significant differences (LSD) analyses ($P\leq 0.05$) were carried out using the mixed procedure of the SAS program package to compare the difference of temperature treatment, the time effect, tracer difference, and the blockade effect.

2.5. [^{11}C]MRB Metabolite Analysis in BAT

BAT tissue samples were firstly homogenized and denatured with equivalent volume of acetonitrile followed with a half amount of saline rinse, and then the mixtures were centrifuged for 5 min at 14,000 rpm to precipitate proteins. Activity in the supernatant from the BAT tissue and that from the saline standard (saline spiked with activity) were monitored and up to 1.0 mL of sample was injected onto the reverse-phase HPLC system (Shimadzu, Kyoto, Japan) consisting of a Luna Phenyl hexyl analytical column (4.6 × 250 mm, 5 mm, Phenomenex, Torrance, CA, USA), and a Flow Cell gamma detector (Raytest, Straubenhardt, Germany). The column was eluted with a mixture of acetonitrile and aqueous 0.1 M ammonium formate in the ratio of 34:66 at a flow rate of 1.6 mL/min with a retention time of the parent compound at 8 min. All the HPLC eluent was fraction-collected with an automated fraction collection device (CF-1 Fraction Collector, Spectrum Chromatography, Houston, TX, USA) in 2-min intervals and counted with the aforementioned automatic gamma counter. The counts of fractions were volume and decay corrected. [^{11}C]MRB metabolite profile in BAT at 40 min post injection was calculated as the ratio of the sum of radioactivity in the fraction containing the parent compound to the total amount of radioactivity collected.

3. Results

3.1. Radiotracers

The average injected dose of [^{11}C]MRB was 10.24 ± 7.44 and 30.34 ± 1.57 MBq with an average specific radioactivity of 83.74

±31.29 MBq/nmol at the time of injection in *ex vivo* biodistribution study, and PET imaging study, respectively. The average injected doses of [^{18}F]FDG were 2.217±0.897 MBq and 10.73 MBq in *ex vivo* biodistribution study and PET imaging study, respectively.

3.2. PET Imaging

PET imaging clearly demonstrated intense [^{11}C]MRB uptake in the interscapular BAT of both room temperature control (SUV of 2.9) and cold-exposed rats (SUV of 3.3), and this BAT labeling was remarkably reduced by pretreatment with unlabeled MRB (Fig. 1). In contrast, [^{18}F]FDG in BAT was only detected in rats treated with cold (SUV of 5.2). In the control group, BAT exhibited only faint to mild [^{18}F]FDG uptake, which was almost indistinguishable from the surrounding tissue uptake, whereas the heart showed the expected intense [^{18}F]FDG uptake similar to that of the cold-treated group.

3.3. Ex vivo biodistribution in awake rats

Time course evaluation revealed similar retention from 20 to 60 min after tracer administration of either [^{18}F]FDG or [^{11}C]MRB in both non-stimulated (basal state) and activated BAT (after cold exposure), or in heart, which is a NET enriched region (Fig. 2); thus, the sampling time parameter was not considered for the statistical analysis. In contrast, significant fast clearance with time was observed in tissues with non-specific [^{11}C]MRB uptake, i.e. WAT (45.8% decrease, $P=0.0068$), skeletal muscle (41.4% decrease, $P=0.0478$), and lung (45.8% decrease, $P=0.0028$) (data were calculated from 20 to 60 min post-injection even though very low activities were detected in both WAT and skeletal muscle in the entire course).

Cold-stimulating uptake of [^{18}F]FDG in BAT was more than 8-fold higher in comparison with non-stimulated control ($P=0.0009$, Table 1) while a small and nonsignificant increase of [^{11}C]MRB uptake was observed in BAT ($P=0.57$). However, the difference of % ID/g of tissue in response to cold appeared to be considerable ($P=0.0817$) for [^{11}C]MRB when assessed with the paired difference t test. The cold-responsive [^{11}C]MRB uptake in BAT was 69% increase in average. At the basal state, the uptake of [^{11}C]MRB in BAT was three times higher than [^{18}F]FDG which was concordant with our imaging findings. The impact of cold exposure on [^{18}F]FDG-PET was significant as expected. In addition to BAT, a significant increase of [^{18}F]FDG uptake in response to cold was also detected in the skeletal muscle ($P=0.0286$) with a 60% increase. In contrast, cold exposure lowered metabolic activity in several organs, including brain (26.2% decrease, $P=0.0142$), pancreas (35.3% decrease, $P=0.0337$), bone (24.5% decrease, $P=0.0263$), and lung (49.6% decrease, $P=0.0656$), perhaps due to differences in the input function. The total activity derived from [^{18}F]FDG and its metabolites also significantly declined with time in blood (60.1% decrease, $P=0.0119$), liver (60.9% decrease, $P=0.0106$), and kidney (36.9% decrease, $P=0.0429$) (data were calculated from 20 to 60 min post-injection). Interestingly, there was no significant thermal effect on [^{11}C]MRB uptake in major organs evaluated in this study.

At the basal state, the uptake of [^{18}F]FDG into tissues with elevated metabolism, e.g. brain ($P < 0.0001$), heart ($P < 0.0001$), kidney ($P=0.0124$ confounded with sampling time) and bone ($P < 0.0001$) appeared to be significantly higher than the uptake of [^{11}C]MRB; alternatively, the uptake of [^{18}F]FDG seemed to be lower in BAT ($P=0.0088$), lung ($P=0.0006$), liver ($P=0.0255$), and pancreas ($P=0.0095$) compared with that of [^{11}C]MRB (Fig. 3).

Pretreatments with unlabeled MRB or with nisoxetine clearly demonstrated substantial NET-specific uptake of [^{11}C]MRB in BAT with a decrease in %ID/g of 85% ($P=0.0013$, Fig. 4) at both room temperature and cold conditions. Large reductions in [^{11}C]MRB retention in NET-rich regions, including heart (70.7% and 69.4% decrease for unlabeled MRB and nisoxetine, respectively, $P=0.003$) and brain (30.3% and 38.6% decrease for unlabeled MRB and nisoxetine, respectively, $P=0.0574$) after NET blockade were also detected.

3.4. [^{11}C]MRB metabolite analysis in BAT

HPLC analysis revealed that 94%–99% of total radioactivity in BAT at 40 min post injection represented unchanged [^{11}C]MRB. Less than 1% of radio-impurity was determined from our spiked [^{11}C]MRB saline sample.

4. Discussion

Using an animal model in which the BAT can be dissected after imaging is completed provides us with a unique opportunity (not possible in humans) to quantify BAT dimensions and mass and to correlate them with the NET-PET imaging results. Significantly higher [^{11}C]MRB uptake in BAT of non-stimulated (room temperature) rats in comparison with [^{18}F]FDG uptake ($P=0.0286$) suggests that [^{11}C]

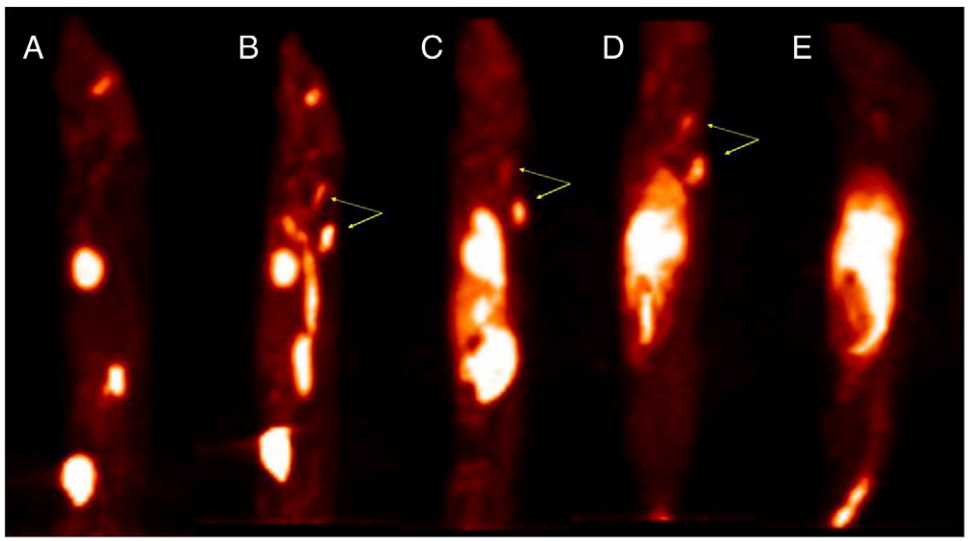

Fig. 1. PET images (50–70 min post-injection) on isoflurane-anesthetized rats from left to right: (A) [^{18}F]FDG room temperature control, (B) [^{18}F]FDG cold-exposed rat, (C) [^{11}C]MRB room temperature control, (D) [^{11}C]MRB cold-exposed rat, and (E) [^{11}C]MRB following blockade by unlabeled MRB. BAT is denoted by arrows. The amounts of injected activity from left to right were 10.73, 10.878, 29.23, 31.45 and 40.875 MBq.

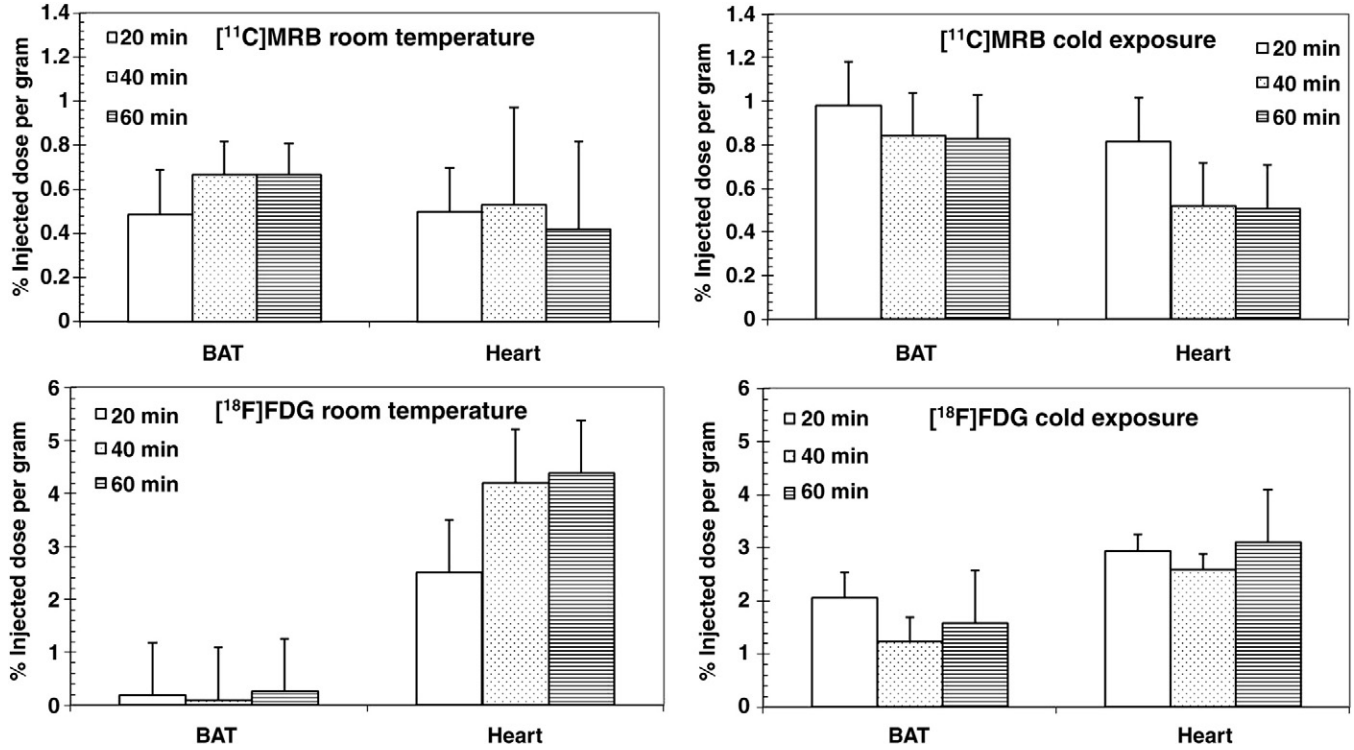

Fig. 2. Time course assessment at 20 (empty bars), 40 (dotted bars) and 60 min (lined bars) after tracer administration of either [^{11}C]MRB or [^{18}F]FDG at both non-stimulated (basal state, room temperature) and cold-exposed (4 °C) conditions in BAT and heart from *ex vivo* studies. Data are shown as mean %ID/g of tissue ± SE ($n = 3$).

MRB may be a better ligand to visualize BAT mass and distribution at the basal state with PET. Our PET imaging studies indicated that [^{11}C]MRB uptake in rats was detected in the interscapular depot which is also the most common location for metabolically active BAT in addition to paravertebral regions. The *ex vivo* biodistribution study showed that BAT was the organ with the 2nd highest uptake of [^{11}C]MRB in rats; less than the uptake in the lung (Table 1). Significant reduction of specific [^{11}C]MRB retention in BAT (85% decrease, $P = 0.0013$), heart (70% decrease, $P = 0.0003$), and brain (34.3% decrease, $P = 0.0574$) after NET blockade demonstrated [^{11}C]MRB uptake in BAT in a localized and NET-specific manner. Moreover, our determination of the chemical composition profile also showed that the main source of activity (94%–99%) in BAT represented the parent tracer [^{11}C]MRB, not its metabolites. This finding is critical for interpretation of BAT images.

The presence of NET-specific [^{11}C]MRB uptake in BAT and heart suggests [^{11}C]MRB could be used to visualize NET-rich regions, a regulated network of NE synapses. NET-specific retention in these organs has also been labeled using [^{11}C]HED, an analog of NE, by Thackeray et al. [19]. The specificity of NET uptake of BAT and heart as determined by NET blockade was significant in both studies while such blocking effect was also observed in brain ($P = 0.0574$, our study), lung and pancreas [19]. Interestingly, [^{11}C]HED seems to be specifically retained in lung in their study; on the other hand, the [^{11}C]MRB uptake appears to be a non-specific accumulation as reported in previous baboon studies [16] and in a fast clearance pattern with time ($P = 0.0028$) in this study. The difference might be due to different doses and routes of administration of the blocking drug (nisoxetine): 2 mg/kg (intravenous) vs. 10 mg/kg (intraperitoneal) and/or due to the different fundamental pharmaceutical properties of these two tracers. On the other hand, a high lung uptake in human of another MRB derivative, (S,S)-[^{18}F]FMeNER-D2, was reported [20]. Its high lung accumulation was considered to be non-specific due to high-affinity amine binding sites in the macrophages in the lungs. The

Table 1
[^{18}F]FDG and [^{11}C]MRB uptake in rat tissues in response to cold exposure.

	[^{18}F]FDG			[^{11}C]MRB	
	Control	Cold exposure	Fold change*	Control	Cold exposure
BAT	0.20 ± 0.05^{a}	1.62 ± 0.30^{c}	$+10.81 \pm 2.67$	0.63 ± 0.09^{b}	0.87 ± 0.18^{b}
WAT	0.06 ± 0.01	0.04 ± 0.006		0.04 ± 0.004	0.04 ± 0.005
Brain	1.11 ± 0.08^{a}	0.81 ± 0.06^{b}	-0.23 ± 0.07	0.14 ± 0.02^{c}	0.16 ± 0.01^{c}
Heart	3.70 ± 0.49^{a}	2.88 ± 0.22^{a}		0.47 ± 0.06^{b}	0.57 ± 0.08^{b}
Muscle	0.12 ± 0.01^{a}	0.18 ± 0.02^{b}	$+0.63 \pm 0.28$	0.09 ± 0.01^{a}	0.10 ± 0.01^{a}
Blood	0.18 ± 0.05	0.13 ± 0.03		0.12 ± 0.03	0.08 ± 0.02
Lung	0.37 ± 0.06^{a}	0.25 ± 0.02^{a}		1.18 ± 0.15^{b}	1.18 ± 0.14^{b}
Liver	0.19 ± 0.05^{a}	0.12 ± 0.02^{a}		0.30 ± 0.03^{b}	0.31 ± 0.04^{b}
Kidney	0.46 ± 0.07^{a}	0.38 ± 0.04^{a}		0.28 ± 0.03^{b}	0.31 ± 0.05^{b}
Bone	0.32 ± 0.03^{a}	0.24 ± 0.02^{b}	-0.21 ± 0.08	0.12 ± 0.02^{c}	0.14 ± 0.02^{c}
Pancreas	0.18 ± 0.02^{b}	0.11 ± 0.01^{a}	-0.30 ± 0.11	0.33 ± 0.04^{c}	0.32 ± 0.03^{c}

Data are shown as mean %ID/g of tissue ± SE ($n = 9$).
BAT: brown adipose tissue; WAT: white adipose tissue.
* Fold change = [(%ID/g cold exposure) − (%ID/g control)] / (%ID/g control). The different superscript letters (a, b, c) and the asterisk signify distinct statistical groups ($P < 0.05$) and statistical significance ($P < 0.05$), respectively.

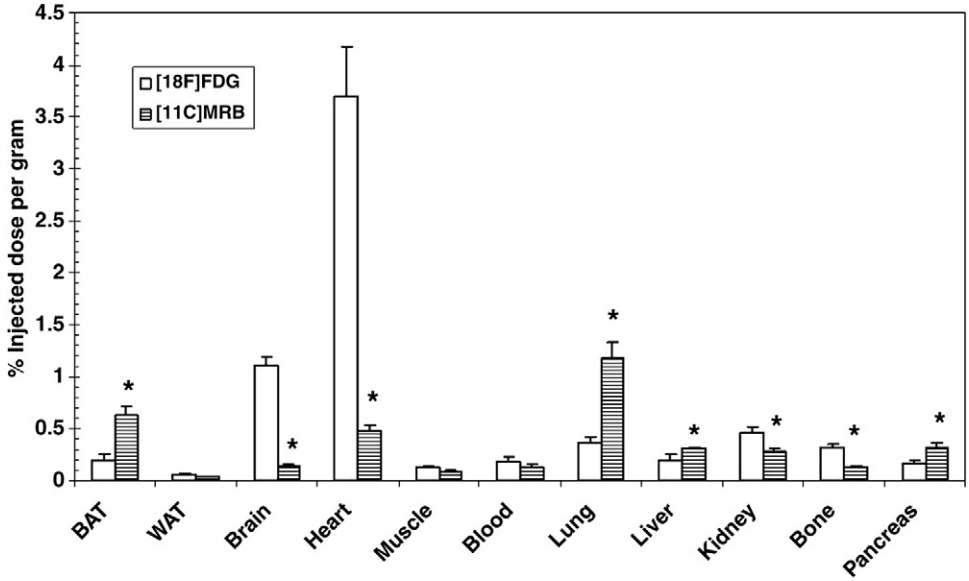

Fig. 3. Comparison of the uptake of [^{18}F]FDG vs. [^{11}C]MRB at the basal state. Note that the uptake of [^{18}F]FDG was lower than that of [^{11}C]MRB in BAT ($P = 0.0088$). Data are shown as mean %ID/g of tissue ± SE. *$P < 0.05$.

uptake of [^{11}C]MRB in WAT and skeletal muscle was low and represented mainly non-specific binding as there was no blocking effect on their uptake after the treatment with nisoxetine or unlabeled MRB. This suggests that these two regions could be potentially used as reference regions for imaging data analysis.

The impact of cold exposure on the [^{18}F]FDG uptake seems to be broader than expected. Besides significant increase of thermogenesis in BAT and skeletal muscles, significant reduction of energy dissipation was also detected in several organs surveyed in this study, i.e. brain, pancreas, bone and lung. Lower brain uptake of [^{18}F]FDG in response to cold was also reported earlier [21]. It will be of interest to follow up whether the decrease of metabolism in those organs leads to reduced brain functions or a lower respiration rate.

There appears to be no significant changes of either metabolism rate (activity level, measured with [^{18}F]FDG) or NET expression (measured with [^{11}C]MRB) in BAT during 20 to 60 min after 4 h of cold exposure supporting that the stimulating condition (4 h at 4 °C) was adequate to trigger BAT to reach its plateau activity [21]. This cold condition which results in a moderate but non-significant increase of [^{11}C]MRB uptake (69%, $P = 0.0817$, $n = 15$) in activated BAT could be due to a change in bioavailability of [^{11}C]MRB or perhaps, either an increase of the affinity of [^{11}C]MRB in BAT membranes or an increase of the available NET density. On the other hand, a significant upsurge of [^{18}F]FDG uptake was observed to levels of 8 and 0.63-fold greater in two major non-shivering thermogenic targets, i.e. BAT and skeletal muscle, respectively.

Our [^{11}C]MRB results correlate well with the findings in female Wistar rats published by Baba et al. [21]. They reported that a signal sent from hypothalamus led to a significant cold-stimulated uptake of [^{123}I]MIBG, a NET tracer, and a cold-induced NET protein expression pattern in BAT. Their immunohistostaining results also indicated that NET can be examined both basally and after mild cold exposure [21]. In comparison to their study, we observed the same significant changes of energy expenditure ([^{18}F]FDG) in response to cold temperature but a smaller increase in NET uptake (69%, $P = 0.0817$, $n = 15$). In addition to the sample variance, the lack of statistical

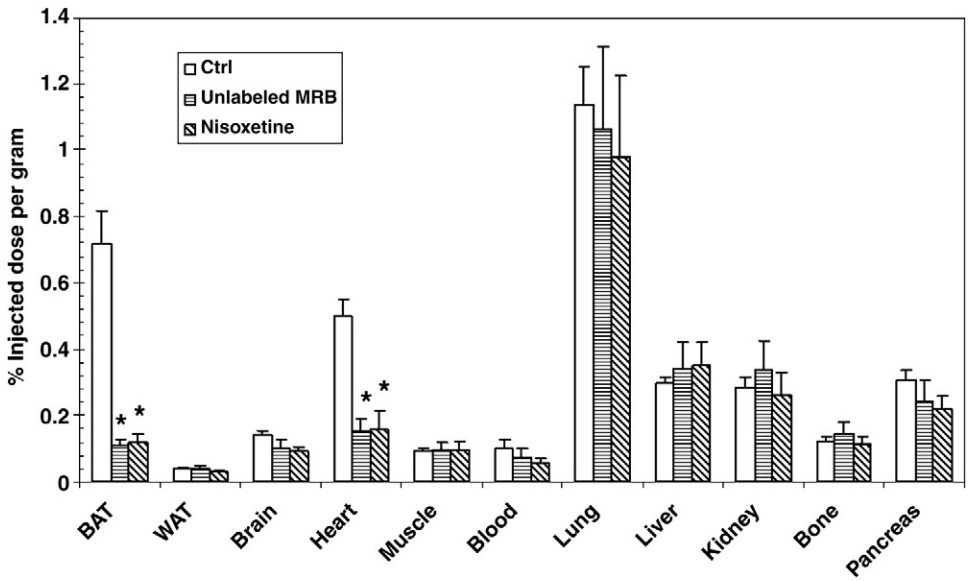

Fig. 4. Significant blocking effect on the [^{11}C]MRB uptake with unlabeled MRB or nisoxetine (2 mg/kg, intravenous injection 30 min prior tracer) was detected in NET-specific retention regions, e.g. BAT and heart. Data are shown as mean %ID/g of tissue ± SE. *$P < 0.05$.

significance might be due to gender and/or strain difference, as well as differences in tracer bioavailability. The potential for gender differences for the NET regulation of cardiac function in humans has previously been shown [22].

Our [^{11}C]MRB data appear to be consistent with the 2 h cold exposure data from King et al. [23], i.e., a moderate increase of NET ligand uptake. In their study, they also showed that a prolonged cold exposure (24 h to 7 days) could result in a decrease in the NET density. Based on the combined data from our [^{18}F]FDG and [^{11}C]MRB studies, one could speculate that a massive SNS stimulation after exposure to the acute cold condition may be effectively enhanced by reducing the overall effect of NET. That is, a relatively reduced effectiveness of NET after cold exposure would help to increase the effective NE in the synapse (or overflow) so that the SNS isn't working so hard; i.e., an improved SNS/metabolic coupling.

Our choice of the [^{11}C]MRB ligand also has other specific advantages. Studies have shown that disruption of NET function directly impacts both autonomic function and mental health [24–27], and that NET function is regulated both centrally and peripherally by insulin [28]. Unlike other potential NET ligands such as[^{18}F]fluorodopamine (a ligand we previously developed that is rapidly metabolized and is not specific to NET) [29,30] or MIBG (a SPECT ligand) [31], [^{11}C]MRB is able to cross the blood brain barrier, allowing for simultaneous central and peripheral imaging. Thus, using [^{11}C]MRB may help to further elucidate mechanisms of BAT action and the role of NET in energy balance of obesity and insulin resistance by simultaneously correlating the CNS (central nervous system) and peripheral SNS functions.

The unexpected, non-malignant high [^{18}F]FDG activity in human BAT has been revealed in the past decade. Our NET-PET approach, unlike [^{18}F]FDG-PET, clearly demonstrated the sensitivity to image BAT distribution under room temperature conditions. Our results suggest that using [^{11}C]MRB may provide an efficient way to localize BAT at room temperature and to eliminate the potential misdiagnosis with [^{18}F]FDG. With the short half-life of ^{11}C (20.4 min), injection of [^{11}C]MRB at room temperature, followed by [^{18}F]FDG injection under cold stimulation, might potentially allow to study BAT function, metabolism, SNS modulation and brain function all at the same time.

5. Conclusions

Our study demonstrates that [^{11}C]MRB can efficiently label BAT at both thermoneutral and thermo-stimulating conditions, and the labeling can be reduced by pretreatment with unlabeled MRB and nisoxetine, demonstrating specific binding of [^{11}C]MRB to the BAT. In contrast, the [^{18}F]FDG labeling occurs under cold conditions only. These results support our hypothesis that NET-PET and FDG-PET imaging of BAT will be highly correlated in adults under mild cold stimulation conditions, and that NET-PET (unlike FDG-PET) will have the sensitivity to image BAT distribution under room temperature conditions.

Acknowledgments

We wish to thank the staff of the Yale PET Center and particularly Nancy Nishimura, Patrick Ouellette, Elisa Rapuano and Joseph Olsen for their technical assistance.

References

[1] Camastra S, Bonora E, Del Prato S, Rett K, Weck M, Ferrannini E. Effect of obesity and insulin resistance on resting and glucose-induced thermogenesis in man. EGIR (European Group for the Study of Insulin Resistance). Int J Obes Relat Metab Disord 1999;23:1307–13.
[2] Golay A, Schutz Y, Felber JP, de Fronzo RA, Jequier E. Lack of thermogenic response to glucose/insulin infusion in diabetic obese subjects. Int J Obes 1986;10:107–16.
[3] Yeckel CW, Gulanski B, Zgorski ML, Dziura J, Parish R, Sherwin RS. Simple exercise recovery index for sympathetic overactivity is linked to insulin resistance. Med Sci Sports Exerc 2009;41:505–15.
[4] Jequier E, Schutz Y. New evidence for a thermogenic defect in human obesity. Int J Obes 1985;9(Suppl. 2):1–7.
[5] Wijers SL, Saris WH. van Marken Lichtenbelt WD. Recent advances in adaptive thermogenesis: potential implications for the treatment of obesity. Obes Rev 2009;10:218–26.
[6] Cypess AM, Lehman S, Williams G, Tal I, Rodman D, Goldfine AB, et al. Identification and importance of brown adipose tissue in adult humans. N Engl J Med 2009;360:1509–17.
[7] Virtanen KA, Lidell ME, Orava J, Heglind M, Westergren R, Niemi T, et al. Functional brown adipose tissue in healthy adults. N Engl J Med 2009;360:1518–25.
[8] Koppen A, Kalkhoven E. Brown vs white adipocytes: the PPARgamma coregulator story. FEBS Lett 2010;584:3250–9.
[9] Saito M, Okamatsu-Ogura Y, Matsushita M, Watanabe K, Yoneshiro T, Nio-Kobayashi J, et al. High incidence of metabolically active brown adipose tissue in healthy adult humans: effects of cold exposure and adiposity. Diabetes 2009;58:1526–31.
[10] van Marken Lichtenbelt WD, Vanhommerig JW, Smulders NM, Drossaerts JM, Kemerink GJ, Bouvy ND, et al. Cold-activated brown adipose tissue in healthy men. N Engl J Med 2009;360:1500.
[11] Logan J, Wang GJ, Telang F, Fowler JS, Alexoff D, Zabroski J, et al. Imaging the norepinephrine transporter in humans with (S, S)-[11C]O-methyl reboxetine and PET: problems and progress. Nucl Med Biol 2007;34:667–79.
[12] Ding YS, Singhal T, Planeta-Wilson B, Gallezot JD, Nabulsi N, Labaree D, et al. PET imaging of the effects of age and cocaine on the norepinephrine transporter in the human brain using (S, S)-[(11)C]O-methylreboxetine and HRRT. Synapse 2010;64:30–8.
[13] Hannestad J, Gallezot JD, Planeta-Wilson B, Lin SF, Williams WA, van Dyck CH, et al. Clinically relevant doses of methylphenidate significantly occupy norepinephrine transporters in humans in vivo. Biol Psychiatry 2010;68:854–60.
[14] Ding Y-, Planeta-Wilson B, Gallezot J-, Lin S-, Williams WA, Carson RE, et al. PET imaging of norepinephrine transporter in adults with attention deficit hyperactivity disorder. J Nucl Med 2010;51(Supplement):330.
[15] Gallezot JD, Weinzimmer D, Nabulsi N, Lin SF, Fowles K, Sandiego C, et al. Evaluation of [(11)C]MRB for assessment of occupancy of norepinephrine transporters: studies with atomoxetine in non-human primates. Neuroimage 2010.
[16] Ding YS, Lin KS, Garza V, Carter P, Alexoff D, Logan J, et al. Evaluation of a new norepinephrine transporter PET ligand in baboons, both in brain and peripheral organs. Synapse 2003;50:345–52.
[17] Okuyama C, Sakane N, Yoshida T, Shima K, Kurosawa H, Kumamoto K, et al. (123)I- or (125)I-metaiodobenzylguanidine visualization of brown adipose tissue. J Nucl Med 2002;43:1234–40.
[18] Tatsumi M, Engles JM, Ishimori T, Nicely O, Cohade C, Wahl RL. Intense (18)F-FDG uptake in brown fat can be reduced pharmacologically. J Nucl Med 2004;45:1189–93.
[19] Thackeray JT, Beanlands RS, Dasilva JN. Presence of specific 11C-meta-hydroxyephedrine retention in heart, lung, pancreas, and brown adipose tissue. J Nucl Med 2007;48:1733–40.
[20] Takano A, Halldin C, Varrone A, Karlsson P, Sjoholm N, Stubbs JB, et al. Biodistribution and radiation dosimetry of the norepinephrine transporter radioligand (S, S)-[18F]FMeNER-D2: a human whole-body PET study. Eur J Nucl Med Mol Imaging 2008;35:630–6.
[21] Baba S, Engles JM, Huso DL, Ishimori T, Wahl RL. Comparison of uptake of multiple clinical radiotracers into brown adipose tissue under cold-stimulated and nonstimulated conditions. J Nucl Med 2007;48:1715–23.
[22] Schroeder C, Adams F, Boschmann M, Tank J, Haertter S, Diedrich A, et al. Phenotypical evidence for a gender difference in cardiac norepinephrine transporter function. Am J Physiol Regul Integr Comp Physiol 2004;286:R851–6.
[23] King VL, Dwoskin LP, Cassis LA. Cold exposure regulates the norepinephrine uptake transporter in rat brown adipose tissue. Am J Physiol 1999;276:R143–51.
[24] Ganguly PK, Dhalla KS, Innes IR, Beamish RE, Dhalla NS. Altered norepinephrine turnover and metabolism in diabetic cardiomyopathy. Circ Res 1986;59:684–93.
[25] Haenisch B, Linsel K, Bruss M, Gilsbach R, Propping P, Nothen MM, et al. Association of major depression with rare functional variants in norepinephrine transporter and serotonin1A receptor genes. Am J Med Genet B Neuropsychiatr Genet 2009;150B:1013–6.
[26] Hahn MK, Blackford JU, Haman K, Mazei-Robison M, English BA, Prasad HC, et al. Multivariate permutation analysis associates multiple polymorphisms with subphenotypes of major depression. Genes Brain Behav 2008;7:487–95.
[27] Hahn MK, Steele A, Couch RS, Stein MA, Krueger JJ. Novel and functional norepinephrine transporter protein variants identified in attention-deficit hyperactivity disorder. Neuropharmacology 2009;57:694–701.
[28] Robertson SD, Matthies HJ, Owens WA, Sathananthan V, Christianson NS, Kennedy JP, et al. Insulin reveals Akt signaling as a novel regulator of norepinephrine transporter trafficking and norepinephrine homeostasis. J Neurosci 2010;30:11305–16.
[29] Ding YS, Fowler JS, Dewey SL, Logan J, Schlyer DJ, Gatley SJ, et al. Comparison of high specific activity (−) and (+)-6-[18F]fluoronorepinephrine and 6-[18F]fluorodopamine in baboons: heart uptake, metabolism and the effect of desipramine. J Nucl Med 1993;34:619–29.
[30] Ding YS, Fowler JS, Gatley SJ, Logan J, Volkow ND, Shea C. Mechanistic positron emission tomography studies of 6-[18F]fluorodopamine in living baboon heart: selective imaging and control of radiotracer metabolism using the deuterium isotope effect. J Neurochem 1995;65:682–90.
[31] Hadi M, Chen CC, Whatley M, Pacak K, Carrasquillo JA. Brown fat imaging with (18)F-6-fluorodopamine PET/CT, (18)F-FDG PET/CT, and (123)I-MIBG SPECT: a study of patients being evaluated for pheochromocytoma. J Nucl Med 2007;48:1077–83.